SEECCM III
3rd South-East European Conference on Computational Mechanics-
an ECCOMAS and IACM Special Interest Conference
M. Papadrakakis, M. Kojic, I. Tuncer (eds.)
Kos Island, Greece, 12–14 June 2013

NONLINEAR FRACTURE ANALYSIS OF CARBON NANOTUBES WITH STONE-WALES DEFECTS

Cengiz Baykasoglu[1], Esra Icer[1] , Alper T. Celebi[1] and Ata Mugan[1]

[1]: Istanbul Technical University, Faculty of Mechanical Engineering, 34437, Istanbul, Turkey

e-mails: baykasoglu@itu.edu.tr, [*]icere@itu.edu.tr, celebial@itu.edu.tr, e-mail: mugan@itu.edu.tr

Keywords: Carbon Nanotubes, Stone–Wales defect, Fracture, Molecular Mechanics, Finite Element Method.

Abstract. *In this paper, a molecular mechanic based finite element model is employed to investigate the effects of Stone-Wales defects on mechanical properties of armchair and zigzag carbon nanotubes by considering large deformation and nonlinear geometric effects. Nonlinear characteristic of the covalent bonds are obtained by using the modified Morse potential and effects of the large deformation and geometric nonlinearities are considered by updating the atomistic coordinates of the original nanotube structure at each load step. The results show that the fractures of all types of carbon nanotubes are brittle, but armchair nanotubes are stiffer than zigzag nanotubes and these defects significantly affect the mechanical performance of nanotubes. Fracture initiation and crack propagation direction issues are also studied. It is shown that the direction of crack propagation in armchair nanotube is in the maximum shear directions having an angle of ±45° along its circumference. Comparisons are made with the failure stress and strain results reported in literature that show good agreement with our results.*

1 INTRODUCTION

Carbon nanotubes (CNTs) have been extensively studied since their discovery in 1991 by Iijima due to their extraordinary mechanical, electronic and thermal properties [1,2]. The mass production of perfect CNTs is very challenging and experimental observations show that some defects such as Stone-Wales (SW or 5-7-7-5) and vacancy defects commonly exist in CNTs. These defects may be induced due to mechanical strain or may emerge during the growth and purification processing [3] and directly affects the mechanical behavior of CNTs [4]. Hence, prediction of mechanical behavior of CNTs having defects is very important and useful in the design of materials having nanotube structures.

Experimental measurements and computational simulations are commonly used to investigate the failure behavior of CNTs. Yu et al. [5] experimentally measured the tensile strength and failure strain of multi-walled carbon nanotubes (MWCNTs) and found 11–63 GPa for the failure strengths and 10–13% for the failure strains. These strain and stress values are significantly smaller than the computational simulation results in literature and these differences can be explained by the presence of defects and some slippage in the attachments which may occur at high-strain cases [6]. Quantum mechanics (QM), molecular dynamics (MD) and molecular mechanic (MM) simulations are widely used to determine the effects of SW defects on the mechanical properties of CNTs in literature [7-13]. Troya et al. [7] used QM methods and observed that SW defects cause a reduction in failure stress such as the reduction of (5,5) tube containing an aggregation of five SW defects range from 6.3% to 53.5%. Chandra et al. [8] studied the local elastic properties of CNTs in the presence of SW defects and observed the stiffness due to defects is reduced by about 30-50 % depending on chirality, tube diameters and loading conditions. Mielke et al. [9] used QM and MD methods and predicted that the presence of SW defects obviously reduce the fracture stress and strain values of CNTs. Belytschko et al. [10] investigated the fracture behavior of defected and non-defected CNTs and reported that the fracture is almost independent from the dissociation energy and depends primarily on the inflection point of the interatomic potential. The brittle fracture is observed and crack grow direction is found in the direction of maximum shear for a SW defected (40,40) armchair nanotube in [10]. Tserpes et al. [11] proposed an atomistic-based progressive fracture model and investigated the SW defects on fracture of SWCNTs by using commercial FE software. The reduction in failure stress and strain predicted ranging from 18 to 25 % and 30 to 41 %, respectively in [11]. Xiao et al. [12] developed an atomistic based finite bond element model for the prediction of fracture behavior SWCNTs and the reduction in failure stress is predicted ranging from 12 to 32 % in the presence of SW defects. Xiao et al. [13] also studied the tensile behaviors of carbon nanotubes with multiple Stone-Wales defects. We investigated nonlinear fracture behavior of vacancy and SW defected single layer graphene sheets (SLGSs) in [14] and developed coupled molecular/continuum mechanical model for SLGSs to enable solving large scale static and fracture problems of SLGSs [15].

In this paper, a molecular mechanic based finite element models are developed to investigate the effects of SW defects in mechanical properties of armchair and zigzag carbon nanotubes. Although progressive fractures of SLCNTs are studied earlier, they are obtained without consideration of geometric nonlinear effects. However, the fracture occurs at relatively large strain values; hence, large deformation effects and geometric nonlinearities have to be considered. The effects of large deformation and geometric nonlinearities are considered by using the modified Morse potential and updating the atomistic coordinates of the original nanotube structure at each load step. The results show that the fractures of all types of carbon nanotubes are brittle and SW defects negatively affect the mechanical performance of the

nanotubes. Comparisons are made with the failure stress and strain results reported in literature which show parallelism with our results.

2 NONLINEAR PROGRESSIVE FRACTURE MODEL OF SWCNTs

2.1 FE formulation of the covalent bonds

When CNTs are subjected to external forces, positions of the atomic nuclei are controlled by the covalent bonds between the C-C atoms. Hence, the deformation pattern of CNTs is very similar to the deformation of frame structures. To this end, C-C bond behavior is simulated by using the Euler-Bernoulli (EB) beam element formulation [16]. The EB beam element parameters are obtained by using harmonic expressions for potential energy terms [17, 18]. The non-linear characteristics of EB beam elements are obtained by using the modified Morse potential. We coded our own SWCNT FE models by using Matlab® and large deformation and nonlinear geometric effects are taken into account. At each load step, initial displacement is applied incrementally on SWCNTs and atomistic coordinates of the original SWCNT structures are updated. According to the modified Morse potential, the potential energy can be expressed as

$$U_{total} = \Sigma U_r + \Sigma U_\theta \tag{1}$$

$$U_r = D_e\left\{\left[1-e^{-\beta(r-r_0)}\right]^2 - 1\right\} \tag{2}$$

$$U_\theta = \frac{1}{2}k_\theta(\theta-\theta_0)^2 + \left[1+k_{sextic}(\theta-\theta_0)^4\right] \tag{3}$$

where U_r is the bond energy due to bond stretching, U_θ is the bond energy due to angle bending, and r and θ are respectively the current bond length and current angle between the adjacent bonds. Values of the parameters in the modified Morse potential functions are taken the same as those in [10]. The stretch force and angle-variation moment can be obtained by differentiation of Equations (2) - (3) as follows

$$F = 2\beta D_e(1-e^{-\beta(r-r_0)})e^{-\beta(r-r_0)} \tag{4}$$

$$M = k_\theta(\theta-\theta_0) + \left[1+3k_{sextic}(\theta-\theta_0)^4\right] \tag{5}$$

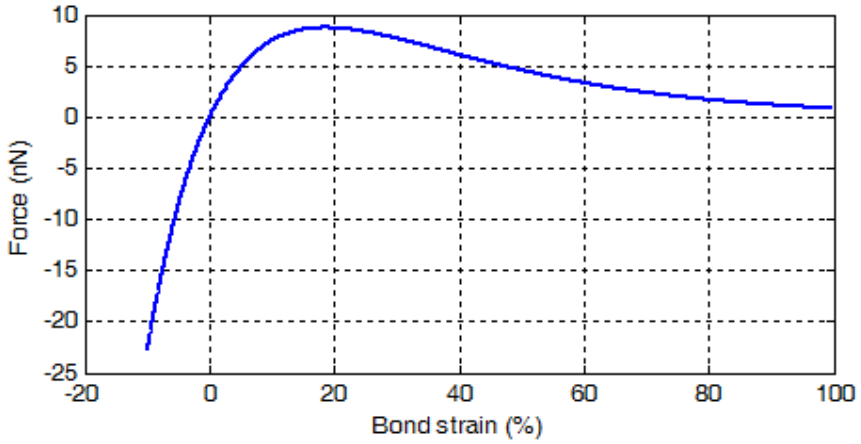

Figure 1: Force-strain curve of the modified Morse potential.

Belytschko et al. [10] reported that the bond angle-bending potential (U_θ) does not contribute to the stretching energy (U_r) and it has little effect on fracture behavior of CNTs. Hence, extra moment effect originating from Equation (5) is neglected. The cut-off distance value of 0.169 nm that corresponds to the inflection point at approximate strain value of 19 % in the modified Morse potential is employed (Figure 1). After the inflection point, the shape of the potential function is not important since material damage occurs [10].

2.2 FE models of SWCNTs

Geometries of different types of defect-free armchair and zigzag nanotube models are constructed by using a Matlab code. Two different types of SWCNTs are considered in the simulations such as (12, 12) armchair and (20, 0) zigzag nanotubes. Sufficiently long SWCNTs are used in simulations to prevent the end effects originating from boundary conditions and SW defects are located in the center of the SWCNTs. When CNTs are subjected to tension loadings, CNTs release its excess tension via formation of topological defects at critical tension value. The SW defect is a topological defect and involves the 90° rotation of a carbon bond about its center and is originally presented as the "SW transformation" [19]. Finally, four hexagons transform into two pentagons and two heptagons. Figure 2 shows schematically the SW formation in the undeformed hexagonal lattice.

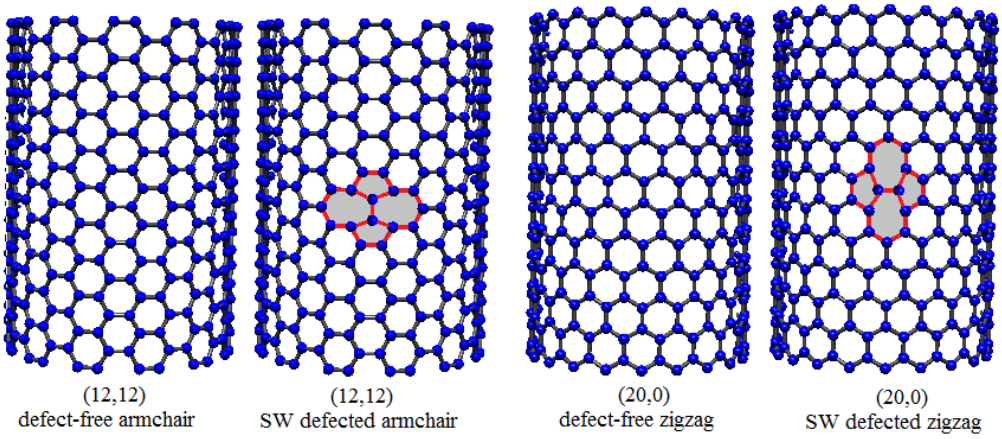

Figure 2: SW defects generated by rationing the C-C bond.

Nardelli et al. [20, 21] showed that defect nucleation in armchair CNTs under transverse tension occurs via SW transformation at critical tensile strain of 5% in CNTs. In addition, Zhang et al. [22] found that this transformation occurs at critical tensile strain of 6% for armchair CNTs and 12% for zigzag CNTs. In this study, strain barrier of 6 % for the armchair and 12 % for the zigzag SWCNTs are considered for the formation of the SW defects. Tserpes et al. [11] used a combination of the stress-strain curve of defect-free and SW-defected CNTs to simulate fracture behavior of SWCNTs. It is assumed in [11] that SWCNT dimensions remain unchanged after the formation of SW defects. Hence, deformation around the defect nucleation region is neglected in [11]. However, after the SW transformation, new configurations of the bonds affect the locations of neighboring atoms which change their locations into new lesser potential energy configurations. On the other hand, Xiao et al. [12, 13] proposed an interaction based mechanics approach to simulate the deformations caused by the formation of SW defects. In our study, to simulate the SW transformation, we started the simulations with defect-free SWCNTs similar to the [11]; then, SW transformation occurs and the configurations of bonds are changed at the defect formation strain; finally, initial pre-strain is applied to

obtain minimized energy configurations of atoms and the simulation is continued until catastrophic failure of the SWCNTs takes place.

3 COMPUTATIONAL RESULTS

All fracture computations of the MM model are completed by using a computer code developed in MATLAB environment. Described by the modified Morse potential, the non-linear behavior of bonds is represented by EB beam elements and an incremental procedure is followed similar to [11] to apply the loading. Initial secant modulus of beam elements (i.e., 6.93 TPa) is obtained through the stress-strain curve of the C-C bond according to the modified Morse potential [14, 15]. In the simulations, all the nodes at one end of SWCNTs are constrained, while the nodes at the other end are subjected to an incremental displacement. The secant modulus and nodal coordinates of each element of the original SWCNT structure is updated at each load step. The secant modulus of each element in the tube structure is set to $F/(A\varepsilon)$ at each load step, where A is the cross sectional area of the element, ε axial strain of the each element, and the interatomic force F is calculated by Equation (4). When the axial strain of a bond reaches to 19 % strain, its stiffness matrix is multiplied by a very small number to simulate the bond break. The strain of SWCNTs is calculated by $\varepsilon_L = (L_s - L_{s0})/L_{s0}$ where L_{s0} is the initial (equilibrium) length and L_s is the current length of the tube. The stress is calculated by $\sigma = F_g/(\pi d t)$ where F_g is the corresponding applied tensile force computed by the summation of the longitudinal reaction forces of the constrained nodes, d is the diameter of tube and t is the thickness of tube. In all calculations, 0.34 nm thickness in [10] is used for SWCNTs.

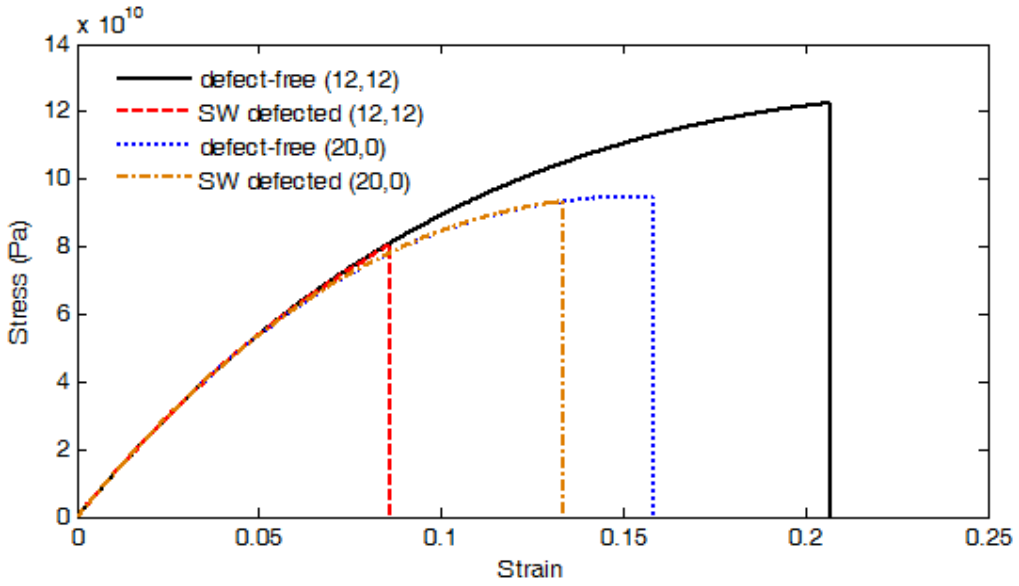

Figure 3: Stress-strain curves of defect-free and SW defected (12,12) and (20,0) SWCNTs under uniaxial load.

Figure 3 shows the calculated stress-strain relationships for defect-free and SW defected armchair (12,12) and zigzag (20,0) SWCNTs without nonlinear geometric effects. As can be seen from Figure 2, the predicted fracture stress and strain values reduce by the presence of SW defects in the structure as expected. As can be seen in Figure 3, the stress- strain curve

exhibits a sudden drop when the stress reaches to the fracture stress, so the fracture is considered to be brittle which are also reported in several studies in literature [5, 10, 12].

Study	Chirality	Defect	ε (%)	σ(GPa)
Present work	12,12	defect-free	21.1	122.8
Present work	12,12	SW	8.58	80.4
Present work	20,0	defect-free	15.9	94.7
Present work	20,0	SW	13.34	93.3
Tserpes et al. [11]	12,12	defect-free	19.61	121.86
Tserpes et al. [11]	12,12	SW	11.96	100
Tserpes et al. [11]	20,0	defect-free	15.75	97.68
Tserpes et al. [11]	20,0	SW	15.75	97.68
Xiao et al. [12]	12,12	defect-free	23.1	126.2
Xiao et al. [12]	12,12	SW	9.8	85.9
Xiao et al. [12]	20,0	defect-free	15.6	94.5
Xiao et al. [12]	20,0	SW	11.0	83.3

Table 1: Predicted failure strain (ε_f) and stress (σ_f) values of SWCNTs.

Table 1 shows the predicted failure strain and stress values of the SWCNTs along with results in literature. It is observed in Table 1 that calculated strain and stress values lie in the same range with the results reported in literature. The predicted fracture stress and strain values of armchair nanotube reduced about 34.5% and 59.3% by the presence of SW defect, respectively. On the other hand, the predicted fracture stress and strain values of zigzag nanotube reduced about 1.5% and 16.1% by the presence of SW defect, respectively. The SW defects resulted in much more reduction in fracture stress and strain values of the armchair SWCNTs than zigzag ones as bond rearrangement causes stress concentration in vertical bonds and early bond fracture occurs.

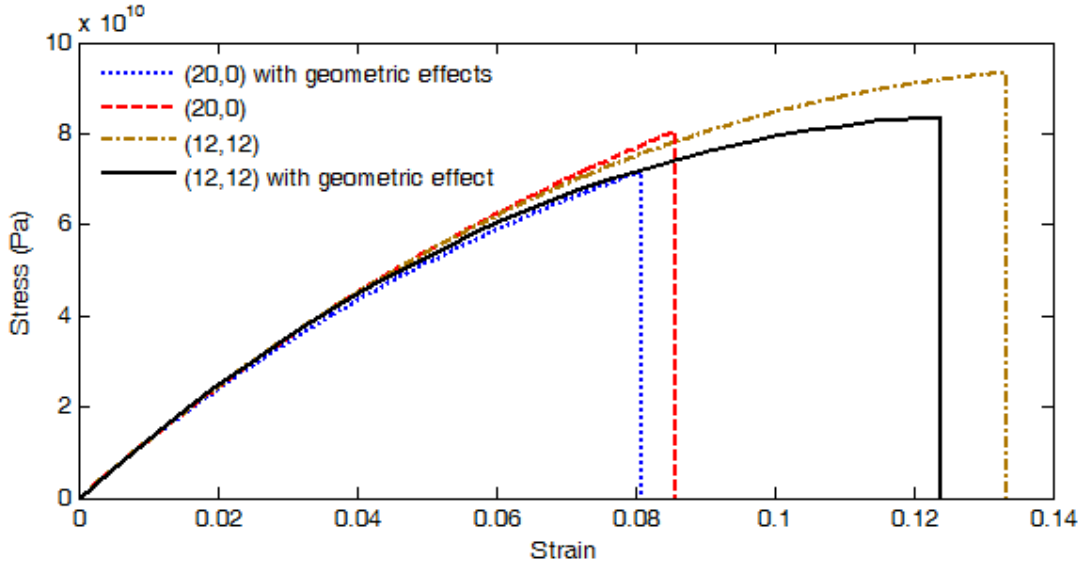

Figure 4: Stress-strain curves of SW defected nanotubes with non-linear geometric effect.

As can be seen in Table 1, Tserpes et al. [11] predicted that fracture stress and strain values of (12,12) armchair SWCNT reduced about 18% and 39%, respectively by the presence of

SW defect, and fracture stress and strain values of defected (20,0) zigzag SWCNT is the same as the zigzag ones. Xiao et al. [12] calculated reduction of fracture stress and strain values of (12,12) armchair SWCNT by the presence of SW defect and found about 32% and 58% for armchair SWCNT and about 12% and 29% for zigzag SWCNT, respectively. In addition, it should be noted that these strain and stress values are significantly smaller than the experimental results in [5] (i.e., range of 11–63 GPa for the failure strengths and 10–13% for the failure strains); these differences can be explained by the presence of defects and some slippage at the attachments which may occur at high-strain cases [6]. The fracture in SWCNTs occurs at relatively large strain values; therefore, we also investigated the effects of geometric nonlinearities on fracture behavior of SW defected SWCNTs. Figure 4 shows the stress-strain curves of SW defected SWCNTs with non-linear geometric effect. The predicted fracture stress and strain values of SW defected armchair SWCNTs reduced about 10.9% and 5.7% considering non-linear geometric effect, respectively. On the other hand, the predicted fracture stress and strain values of SW defected zigzag SWCNTs reduced about 10.3% and 3.5% considering non-linear geometric effects, respectively.

Our proposed approach is able to give the correct prediction of fracture initiation and post failure behavior of SWCNTs. However, modified Morse potential function is not capable of describing the behavior of SWCNTs after the covalent bonds are broken where the reconfiguration of bonds and structural transformations may occur. Figure 5 shows the crack evolution of the SW-defected armchair and zigzag SWCNTs via elimination of broken C-C bonds based on the cut-of distance failure criterion. As can be seen in Figure 5a, the fracture initiated from the vertical bond which connects the two pentagons and continued diagonal crack paths. Then, the crack propagates around the SWCNT in the ±45° direction along its circumference. Similar fracture patterns are also observed in literature [10, 11, 12]. As can be seen in Figure 5b, the fracture initiated from the vertical bonds of the upper heptagon which is shown in dark colour in Figure 5b and propagated circumferentially in the same row. The same crack propagation characteristic has also been observed in literature [11].

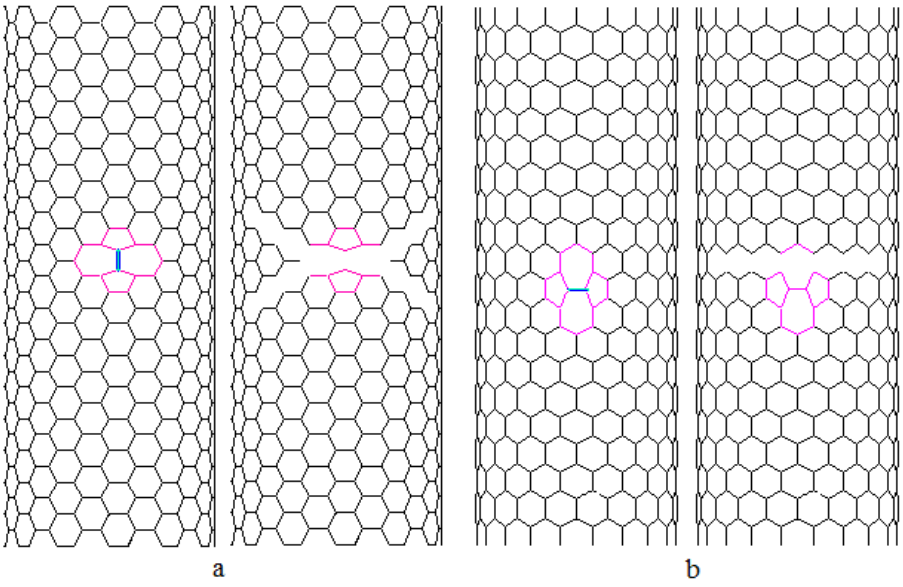

Figure 5: Fracture initiation and propagation directions of the SW- defected SWCNTs; (a) armchair, (b) zigzag SWCNTs.

4 CONCLUSIONS

In this paper, a MM based FE model is developed to predict the effects of Stone-Wales defects on mechanical properties of SWCNTs. The proposed approach includes large deformation and nonlinear geometric effects. Euler-Bernoulli beam elements are used to represent C-C bonds and non-linear characteristic of the beam elements are obtained by using the modified Morse potential. The results show that the fractures of all types of carbon nanotubes are brittle and the SW defects resulted in much more reduction in fracture stress and strain values of the armchair SWCNTs than zigzag ones. Fracture initiation and crack propagation direction issues are also studied. It is shown that crack propagation direction of armchair SWCNT is in maximum shear directions having an angle of ±45° along its circumference, and the fracture initiated from the vertical bonds of the upper heptagon and propagated circumferentially in the same row in case of zigzag SWCNTs. Comparisons are made with the failure stress and strain results reported in literature that show well agreement with our results.

REFERENCES

[1] V.N. Popov, Carbon nanotubes: properties and application. *Materials Science and Engineering: R: Reports*, **43(3)**, 61-102, 2004.

[2] S. Iijima, Helical microtubules of graphitic carbon. *Nature*, **354**, 56-58, 1991.

[3] J.C. Charlier, Defects in Carbon Nanotubes. *Accounts of Chemical Research*, **35**, 1063-1069, 2002.

[4] R.W. Haskins, R.S. Maier, R.M. Ebeling, C.P. Marsh, D.L. Majure, A.J. Bednar et al.,Tight-binding molecular dynamics study of the role of defects on carbon nanotube moduli and failure. *Journal of Chemical Physics*, **127(7)**, 74708–74718, 2007.

[5] M.F. Yu, O. Lourie, M.J. Dyer, K. Moloni, T.F. Kelly, R.S. Ruoff, Strength and breaking mechanism of multiwalled carbon nanotubes under tensile load. *Science*, **287**, 637–40, 2000.

[6] S. Zhang, S.L. Mielke, R. Khare, D. Troya, R.S. Ruoff, G.C. Schatz et al., Mechanics of defects in carbon nanotubes: Atomistic and multiscale simulations. *Physical Review B*, **71**, 115403, 2005.

[7] D. Troya, S.L. Mielke, G.C. Schatz, Carbon nanotube fracture – differences between quantum mechanical mechanisms and those of empirical potentials. *Chemical Physics Letters*, **382**, 133-141, 2003.

[8] N. Chandra, S. Nimilae and C. Shet, Local elastic properties of carbon nanotubes in the presence of Stone-Wales defects. *Physical Review B*, **69**, 94101-1, 2004.

[9] S.L. Mielke, D. Troya, S. Zhang, J-L. Li, S. Xiao, R. Car et al., The role of vacancy defects and holes in the fracture of carbon nanotubes. *Chemical Physics Letters*, **390**, 413-420, 2004.

[10] T. Belytschko, S.P. Xiao, G.C. Schatz, R.S. Ruoff, Atomistic simulations of nanotube fracture. *Physical Review B*, **65**, 235430, 2002.

[11] K.I. Tserpes, P. Papanikos, The effect of Stone-Wales defect on the tensile behavior and fracture of single-walled carbon nanotubes. *Composite Structures*, **79**, 581-589, 2007.

[12] J.R. Xiao, J. Staniszewski, J.W. Gillespie, Fracture and progressive failure of defective graphene sheets and carbon nanotubes. *Composite Structures*, **88**, 602-609, 2009.

[13] J.R. Xiao, J. Staniszewski, J.W. Gillespie, Tensile behaviors of graphene sheets and carbon nanotubes with multiple Stone-Wales defects. *Materials Science and Engineering: A*, **527**, 715-723, 2010

[14] C. Baykasoglu, A. Mugan, Nonlinear fracture analysis of single-layer graphene sheets. *Engineering Fracture Mechanics*, **96**, 241-250, 2012

[15] C. Baykasoglu, A. Mugan, Coupled molecular/continuum mechanical modeling of graphene sheets. *Physica E*, **45**, 151-161, 2012

[16] G.R. Liu and S.S. Quek, *The finite element method A practical course*, Butterworth-Heinemann, Oxford, 2003.

[17] C. Li, T.W. Chou, A structural mechanics approach for the analysis of carbon nanotubes. *International Journal Solids Structures*, **40**, 2487–2499, 2003.

[18] K.I. Tserpes, P. Papanikos, Finite element modeling of single-walled carbon nanotubes. *Composites Part B*, **36**, 468–477, 2005.

[19] A.J. Stone and D.J. Wales, Theoretical studies of icosahedral C60 and some related species. *Chemical Physics Letters.* **128(5–6)**, 501–3, 1986.

[20] M.B. Nardelli, B.I. Yakobson and J. Bernholc, Mechanism of strain release in carbon nanotubes. *Physical Review B*, **57**, R4277-R4280, 1998.

[21] M.B. Nardelli, B.I. Yakobson and J. Bernholc, Brittle and Ductile Behavior in Carbon Nanotubes. *Physical Review Letters*, **81**, 4656-4659, 1998.

[22] P. Zhang P, P.E. Lammert and V.H. Crespi, Plastic deformations of carbon nanotubes *Physical Review B*, **81**, 5346–5349, 1998.